Experimental cross section study of ^{40}Ca + ^{175}Lu: Searching for new neutron-deficient Pa isotopes

M. M. Zhang,[1] Z. Y. Zhang,[1,2] Z. G. Gan,[1,2,3,*] N. Wang,[4,5,†] H. Yao,[4,5] J. G. Wang,[1] M. H. Huang,[1,2,3] L. Ma,[1,3] H. B. Yang,[1] C. L. Yang,[1] Y. L. Tian,[1,3] Y. S. Wang,[1,3] J. Y. Wang,[1] Y. H. Qiang,[1] X. L. Wu,[1] S. Y. Xu,[1,2] X. Y. Huang,[1,2] Z. C. Li,[1,2] Z. Zhao,[1,2] L. C. Sun,[4,1] H. Zhou,[1,2] X. Zhang,[1,2] G. Xie,[1,2] L. Zhu,[1,2] J. H. Zheng,[1,2] Y. J. Li,[6] F. Guan,[4,1] Z. W. Lu,[1] W. X. Huang,[1,2,3] Y. He,[1,2,3] H. S. Xu,[1,2] Z. Z. Ren,[7] and S. G. Zhou[8,9]

[1]*CAS Key Laboratory of High Precision Nuclear Spectroscopy, Institute of Modern Physics, Chinese Academy of Sciences, Lanzhou 730000, China*

[2]*School of Nuclear Science and Technology, University of Chinese Academy of Sciences, Beijing 100049, China*

[3]*Advanced Energy Science and Technology Guangdong Laboratory, Huizhou 516029, China*

[4]*Department of Physics, Guangxi Normal University, Guilin 541004, China*

[5]*Guangxi Key Laboratory of Nuclear Physics and Technology, Guilin 541004, China*

[6]*Shandong Provincial Key Laboratory of Optical Astronomy and Solar-Terrestrial Environment, School of Space Science and Physics, Shandong University, Weihai 264209, China*

[7]*School of Physics Science and Engineering, Tongji University, Shanghai 200092, China*

[8]*CAS Key Laboratory of Theoretical Physics, Institute of Theoretical Physics, Chinese Academy of Sciences, Beijing 100190, China*

[9]*Center of Theoretical Nuclear Physics, National Laboratory of Heavy-Ion Accelerator, Lanzhou 730000, China*

(Received 16 October 2023; accepted 21 November 2023; published 9 January 2024)

The fusion-evaporation reaction ^{40}Ca + ^{175}Lu aimed at synthesizing new neutron-deficient protactinium isotopes has been studied at the gas-filled recoil separators SHANS and SHANS2. The cross sections for the *xn* and *pxn* evaporation channels were measured. The calculation by the statistical model HIVAP was performed to reproduce the experimental data. The quasifission process in the ^{40}Ca + ^{175}Lu reaction was also studied with time-dependent Hartree-Fock theory and the improved quantum molecular dynamics model. It is shown that the influence of quasifission in the analysis of evaporation residue cross sections of this reaction can be neglected.

DOI: 10.1103/PhysRevC.109.014608

I. INTRODUCTION

Synthesizing new nuclides far from the line of β stability and studying their decay properties are interesting subjects in present-day nuclear physics. For the production of nuclei above the $Z = 82$ shell and near the $N = 126$ shell, heavy-ion induced fusion-evaporation reaction is used as an effective method [1–3]. However, since the fission barriers are low and the compound nuclei are typically produced with excitation energies of several tens of MeV, the cross sections for the production of evaporation residues in these reactions would reach down to nanobarn levels or even less [4–6]. Fortunately, with the advent of high-intensity heavy-ion accelerators together with the development of recoil separators, several new neutron-deficient nuclei in this region have been successfully synthesized in recent years [6–10].

In this work, the fusion-evaporation reaction ^{40}Ca + ^{175}Lu for the synthesis of new neutron-deficient protactinium isotopes was studied. The cross sections of *xn* and *pxn* evaporation channels were measured and compared with HIVAP calculations. The quasifission process of ^{40}Ca + ^{175}Lu was also studied with time-dependent Hartree-Fock (TDHF) theory and the improved quantum molecular dynamics (ImQMD) model.

II. EXPERIMENTAL DETAILS

The ^{40}Ca + ^{175}Lu reaction was studied in two separate experiments. In the first experiment, the ^{40}Ca beam was delivered by a linear accelerator, namely the China Accelerator Facility for Superheavy Elements (CAFE2) [11,12]. The incident beam energies were 212 MeV and 228 MeV and the beam intensities were up to a maximum of 2.5 pμA. 20 arc-shaped ^{175}Lu targets with a thickness of 0.45 mg/cm^2 were mounted on a rotating wheel of 50-cm diameter and the wheel was rotated at 2000 rpm during the irradiation. The beam intensity and target thickness were monitored by a plastic scintillator with Si-PM (silicon photomultiplier) mounted 45 degrees with respect to the incident beam axis, which counted elastically scattered projectiles. Recoiled evaporation residues (ERs) were separated from the primary beam and other unwanted reaction products by a new gas-filled recoil separator SHANS2 (spectrometer for heavy atoms and nuclear structure-2) [12]. The separator was filled with helium gas at a pressure of 100 Pa and the magnets were set to guide the ERs to the center of the focal plane. ERs surviving during the flight were implanted into a 300-μm-thick double-sided silicon strip detector (DSSD) with 128 vertical and 48 horizontal

*Corresponding author: zggan@impcas.ac.cn
†Corresponding author: wangning@gxnu.edu.cn

1-mm-wide strips. To detect the α particles escaped from the DSSD, six single-sided strip detectors (SSDs) with sensitive areas of $120 \times 63\,\text{mm}^2$ were mounted perpendicular to the surface of the DSSD. Each SSD has a thickness of 500 μm and is divided into eight $15 \times 63\,\text{mm}^2$ side strips. The total detection efficiency of the detector array was measured to be 86(8)%. Two multiwire proportional counters were installed in front of the DSSD allowing us to distinguish the α-decay events from the implantation ones. Behind the DSSD, three punch-through silicon detectors were mounted for the rejection of signals produced by energetic light particles. All the silicon detectors were cooled down to -30°C to gain a better energy resolution using an alcohol cooling system.

In the second experiment, the ^{40}Ca beam with a beam energy of 202 MeV and an intensity of 0.5 pμA was supplied by the Sector Focusing Cyclotron of the Heavy Ion Research Facility in Lanzhou (HIRFL), China. A fixed ^{175}Lu target with a thickness of $0.5\,\text{mg/cm}^2$ was used. The ERs were separated from the beam ions by the gas-filled recoil separator SHANS (spectrometer for heavy atoms and nuclear structure) and implanted into three 300-μm-thick position-sensitive strip detectors (PSSDs) installed side by side at the focal plane of the separator. More details of SHANS and the detector system can be found in Refs [13–15].

30 and 16 waveform digitizers V1724 with 100 MHz sampling from CAEN S.p.A. [16] were used for the data acquisition at SHANS2 and SHANS, respectively. The energy calibrations of silicon detectors were performed using a three-peak (^{244}Cm, ^{241}Am, and ^{239}Pu) α source as well as the known peaks from the nuclei produced in the ^{40}Ca + ^{175}Lu reaction. The typical energy resolution was about 40 keV [full width at half-maximum (FWHM)] for 6–8 MeV α particles detected by the DSSD or PSSDs. The total energy of an escaped α particle was reconstructed by adding the deposited energies in the DSSD and SSDs (or PSSDs + SSDs), and had an energy resolution of 80 keV (or 240 keV for PSSDs + SSDs).

III. RESULTS AND DISCUSSION

Identification of most of the nuclei produced in the ^{40}Ca + ^{175}Lu reaction could be performed using their unique α-decay energy and half-life. As an example, Fig. 1 shows the energy spectrum of the α decays following the implanted residues within 2 s measured in the DSSD at a beam energy of 228 MeV. The complexity of this α spectrum is due to several different evaporation channels with their subsequent α-decay cascades. Nevertheless, the Fr, Ra, and Ac isotopes produced in charged- particle evaporation channels are identified based on their tabulated α-decay properties [17]. For the nuclei produced with relatively low statistics, the method of genetically correlated events was used. In Fig. 2, a two-dimensional scatter plot showing the correlation between the parent and daughter α-particle energies is presented. The searching time windows were 50 ms for the ER-α1 pair and 2 s for α1-α2 pair. The α-decay correlations originated from ^{209}Th, ^{210}Th, ^{206,206m}Ac, and ^{207}Ac isotopes are clearly identified based on their known decay properties [18–20].

The statistics of specific nuclei determined from above-mentioned spectra, together with the information of the target

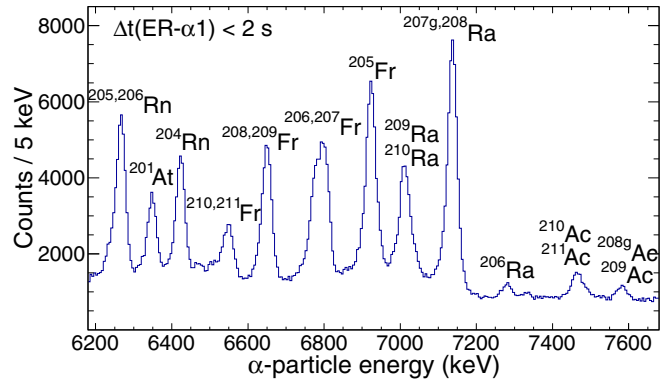

FIG. 1. Energy spectrum for α particles following the implanted residues within a time window of 2 s measured in the ^{40}Ca + ^{175}Lu reaction at a beam energy of 228 MeV.

thickness, beam dose, detection efficiency, and transmission efficiencies of SHANS and SHANS2 were used to deduce the evaporation residue cross sections. The α-decay branching ratio of each nuclei of interest was adopted from Ref. [17]. The transmission efficiencies of SHANS and SHANS2 were measured to be 14% and 47%, respectively, by using the ^{40}Ar + ^{175}Lu reaction [12,13]. The same transmission efficiency was assumed for the *xn* and *pxn* evaporation channels of ^{40}Ca + ^{175}Lu. However, for the α*xn* channel the uncertainty of transmission efficiency is larger due to a broader ER angular distribution after the α-particle emission. The resulting *xn* and *pxn* cross sections for the ^{40}Ca + ^{175}Lu reaction are given in Table I. The effective beam energies at the center of target were calculated using the program SRIM [21]. The error bars of the cross sections only represent statistical errors determined by the method described in Ref. [22]. In some cases, only upper limits for the cross sections are given.

The measured cross sections for the ^{40}Ca + ^{175}Lu reaction can be discussed with regard to the fusion process and to the de-excitation of the compound nucleus. The evaporation residue cross section σ_{ER} is commonly modeled as the product

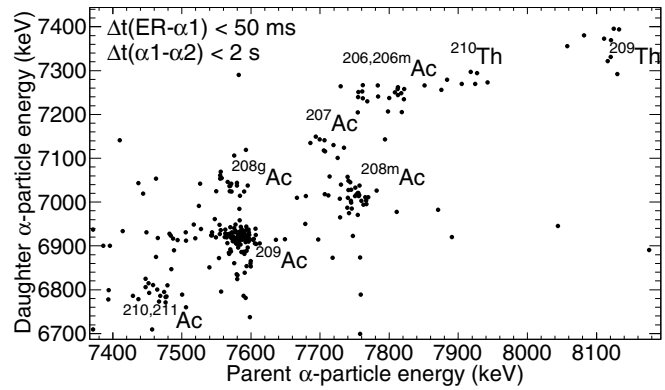

FIG. 2. Two-dimensional scatter plot of parent and daughter α-particle energies for correlated ER-α1-α2 events measured in the ^{40}Ca + ^{175}Lu reaction at a beam energy of 228 MeV. The searching time windows were 50 ms for the ER-α1 pair and 2 s for the α1-α2 pair.

TABLE I. Measured *xn* and *pxn* cross sections for the ^{40}Ca + ^{175}Lu reaction in the present work. $E_{\rm lab,cot}$ is beam energy at the center of the target. $E^*_{\rm CN}$ is the excitation energy of the compound nuclei. The indicated errors represent only statistical uncertainties. In some cases, only upper limits for the cross sections are given.

$E_{\rm lab,cot}$ (MeV)	$E^*_{\rm CN}$ (MeV)	$\sigma_{4n}(^{211}{\rm Pa})$ (pb)	$\sigma_{5n}(^{210}{\rm Pa})$ (pb)	$\sigma_{6n}(^{209}{\rm Pa})$ (pb)	$\sigma_{p3n}(^{211}{\rm Th})$ (pb)	$\sigma_{p4n}(^{210}{\rm Th})$ (pb)	$\sigma_{p5n}(^{209}{\rm Th})$ (pb)
200	55	< 76	–	–	669^{+226}_{-179}	< 76	–
209	62	$2^{+3}_{-1.5}$	7^{+3}_{-2}	–	126^{+17}_{-15}	152^{+17}_{-15}	< 0.8
225	75	–	2^{+3}_{-2}	< 1	< 1	16^{+9}_{-6}	23^{+10}_{-7}

of three factors,

$$\sigma_{\rm ER} = \sigma_{\rm cap} P_{\rm CN} W_{\rm sur}. \quad (1)$$

where $\sigma_{\rm cap}$ is the capture cross section for the transition of the colliding nuclei over the Coulomb barrier, $P_{\rm CN}$ is the probability that the system then evolves into an equilibrated compound nucleus, and $W_{\rm sur}$ is the survival probability of the excited nucleus. The compound nucleus formation probability $P_{\rm CN}$ is hindered by the quasifission of the hot rotating dinuclear system into two fission-like fragments. In this work, the probability of quasifission of the concerned ^{40}Ca + ^{175}Lu reaction is very small and thus $\sigma_{\rm ER} \simeq \sigma_{\rm cap} W_{\rm sur}$. To clarify this, we have studied the ^{40}Ca + ^{175}Lu reaction with TDHF theory [23] and ImQMD model [24]. It is usually thought that in quasifission, the composite system breaks apart before reaching compact equilibrium shapes, often occurring in less than 10 zs [25]. In both TDHF and ImQMD calculations, the reaction systems are self-consistently evolved to $t = 20$ zs. In Fig. 3, we show the time evolution of the density distribution from the TDHF calculations at side and tip orientations for head-on collisions at an incident energy of $E_{\rm c.m.} = 164.8$ MeV. The quasifission is not observed even at $t = 20$ zs. At the same time, we perform 10^5 simulations for ^{40}Ca + ^{175}Lu reaction by using the ImQMD model and find the probabilities of quasifission are smaller than 1% at $E_{\rm c.m.} = 162.7$ MeV and 167.5 MeV. Therefore, in the analysis of evaporation residue cross sections of ^{40}Ca + ^{175}Lu, the influence of quasifission can be neglected.

A standard evaporation calculation was performed for the ^{40}Ca + ^{175}Lu reaction by using the code HIVAP [27,28]. In this model, the fusion mechanism is assumed to occur when the projectile-target system overcomes the interaction barrier, which is calculated using the Bass global nucleus-nucleus potential [26]. The effect of deformation which may be important near the barrier and at sub-barrier energies was included. Moreover, fluctuations of the fusion barrier with a Gaussian distribution were also taken into account. For the de-excitation stage, the HIVAP code makes use of standard evaporation theory by considering the competition between various decay channels, such as neutron, proton, α-particle evaporation, γ-ray emission, and fission. The nuclear level density parameters and fission barriers are the two most sensitive parameters involved in the calculation. For the former, we used the Reisdorf parametrization from Ref. [28]. The fission barriers B_f were calculated with the formula: $B_f = C_f \times B_f^{\rm LD} + \Delta W_{gs}$, where C_f is a free scaling factor, $B_f^{\rm LD}$ is the liquid drop fission barrier [29], and ΔW_{gs} is the ground-state shell correction [30]. The fission barrier scaling factor C_f was the only adjustable in our calculation. In order to check the consistency of the calculation, we performed HIVAP calculations for the ^{40}Ar-induced fusion reactions with isotopes of Lu, Hf, and Ta, in which the evaporation residues produced are adjacent to those of the investigated reaction [4]. We note that good agreement between calculation and experiment results was obtained when the scaling parameter $C_f = 0.70$ was used. Thus, it is reasonable to perform the HIVAP calculation for the ^{40}Ca + ^{175}Lu reaction with the same C_f value. Figure 4 shows the calculation results of HIVAP together with measured data for the *xn* and *pxn* channels of the ^{40}Ca + ^{175}Lu reaction. The uncertainties of measured cross sections are not shown in the figure for clarity. A satisfactory agreement can be found between the calculated and measured data, both in terms of the absolute values and energy dependence of the cross sections. The cross sections for the *pxn* channel were dozens of times higher than those of the *xn* channel. This could be due to the low proton binding energy of the neutron-deficient compound nucleus, which makes the proton emission preferential. For the isotope ^{211}Pa, the production cross section of 2 pb was measured at $E^*_{\rm CN} = 62$ MeV while only an upper limit of 76 pb was obtained at $E^*_{\rm CN} = 55$ MeV. We note that this new isotope was recently synthesized in the ^{181}Ta(^{36}Ar, $6n$)^{211}Pa reaction by employing the gas-filled recoil separator RITU [6]. The measured cross section of 20 pb is comparable to the maximum value predicted by HIVAP calculation for the ^{40}Ca + ^{175}Lu reaction. A dozen α-decay events of a new isotope ^{210}Pa was

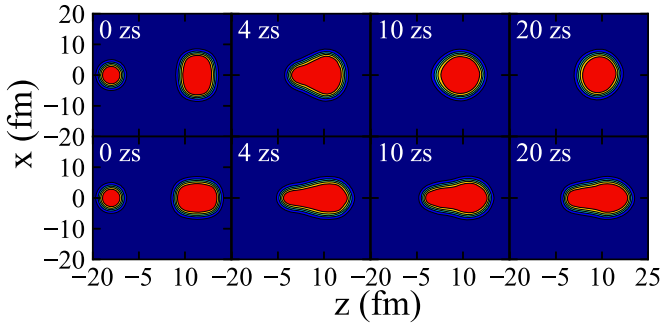

FIG. 3. Time evolution of the mass density in the tip and side orientations for head-on collisions of ^{40}Ca + ^{175}Lu at an incident energy of $E_{\rm c.m.} = 164.8$ MeV.

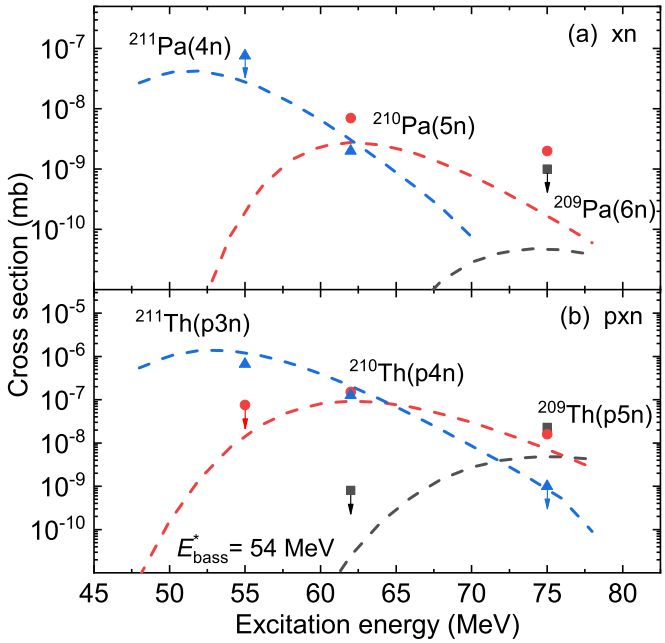

FIG. 4. Cross sections for the fusion-evaporation reaction ^{40}Ca + ^{175}Lu: (a) *xn* channels, (b) *pxn* channels. Experimental data measured in the present work are shown by the symbols. The values calculated using HIVAP ($C_f = 0.70$) are shown by dashed lines. Bass barrier E^*_{bass} is calculated according to Ref. [26].

observed using beam energies of 212 MeV ($E^*_{CN} = 62$ MeV) and 228 MeV ($E^*_{CN} = 75$ MeV) at SHANS2. The detailed α-decay properties of this isotope will be given elsewhere [31]. The beam time is about 76 and 65 h, respectively. The production cross section of this new isotope is reached down to a few picobarns, which demonstrate the high sensitivity of SHANS2 for the production of neutron-deficient heavy and superheavy nuclei. For ^{209}Pa, only an upper limit of cross section of 1 pb was achieved and a maximum of about 0.05 pb was predicted by the HIVAP calculation. Higher beam intensity and more beam time are needed to produce this very neutron-deficient nucleus in a future experiment.

IV. SUMMARY

In conclusion, the fusion-evaporation reaction ^{40}Ca + ^{175}Lu aimed at synthesizing new neutron-deficient Pa isotopes was studied at the gas-filled recoil separators SHANS and SHANS2. The *xn* and *pxn* cross sections were measured at three beam energies. The quasifission process in the ^{40}Ca + ^{175}Lu reaction was studied with TDHF and ImQMD models and the results show that the influence of quasifission in the analysis of evaporation residue cross sections can be neglected. The measured data are compared with the calculation results performed by the standard evaporation code HIVAP. Good agreement between calculated and measured data was obtained when the fission barrier scaling parameter $C_f = 0.70$ was used. The evaporation residue cross sections of ^{40}Ca + ^{175}Lu were measured to be as low as a few picobarns, which demonstrate that SHANS2 is an excellent apparatus for the synthesis of heavy and superheavy nuclei using fusion-evaporation reactions.

ACKNOWLEDGMENTS

The authors would like to thank the accelerator crew of HIRFL and CAFE2 for providing the stable ^{40}Ca beams. This work was supported by the National Natural Science Foundation of China (Grants No. 12105328, 12075286, 12265006), the Strategic Priority Research Program of Chinese Academy of Sciences (Grant No. XDB34010000), the National Key R&D Program of China (Contract No. 2018YFA0404402), the Guangdong Major Project of Basic and Applied Basic Research (Grant No. 2021B0301030006), the CAS Light of West China Program (2022-04), the CAS Project for Young Scientists in Basic Research (Grant No. YSBR-002), and the Youth Innovation Promotion Association CAS (Grants No. 2023439, 2020409).

[1] M. Thoennessen, Discovery of Nuclides Project webpage, https://people.nscl.msu.edu/~thoennes/isotopes/index.html.
[2] V. I. Zagrebaev, Phys. Rev. C **64**, 034606 (2001).
[3] T. A. Werke, C. S. Salas, K. J. Glennon, D. A. Mayorov, E. E. Tereshatov, M. F. Volia, D. M. Wright, and C. M. Folden, Phys. Rev. C **106**, 054615 (2022).
[4] D. Vermeulen, H. G. Clerc, C. C. Sahm, K. H. Schmidt, J. Keller, G. Münzenberg, and W. Reisdorf, Z. Phys. A: At. Nucl. **318**, 157 (1984).
[5] F. Heßberger, S. Hofmann, D. Ackermann, V. Ninov, M. Leino, S. Saro, A. Andreyev, A. Lavrentev, A. Popeko, and A. Yeremin, Euro. Phys. J. A **8**, 521 (2000).
[6] K. Auranen, J. Uusitalo, H. Badran, T. Grahn, P. T. Greenlees, A. Herzáň, U. Jakobsson, R. Julin, S. Juutinen, J. Konki, M. Leino, A.-P. Leppänen, G. O'Neill, J. Pakarinen, P. Papadakis, J. Partanen, P. Peura, P. Rahkila, P. Ruotsalainen, M. Sandzelius *et al.*, Phys. Rev. C **102**, 034305 (2020).
[7] J. Khuyagbaatar, A. Yakushev, C. E. Düllmann, D. Ackermann, L.-L. Andersson, M. Block, H. Brand, D. M. Cox, J. Even, U. Forsberg, P. Golubev, W. Hartmann, R.-D. Herzberg, F. P. Heßberger, J. Hoffmann, A. Hübner, E. Jäger, J. Jeppsson, B. Kindler, J. V. Kratz *et al.*, Phys. Rev. Lett. **115**, 242502 (2015).
[8] J. L. Pore, J. M. Gates, R. Orford, C. M. Campbell, R. M. Clark, H. L. Crawford, N. E. Esker, P. Fallon, J. A. Gooding, J. T. Kwarsick, A. O. Macchiavelli, C. Morse, D. Rudolph, A. Såmark-Roth, C. Santamaria, R. S. Shah, and M. A. Stoyer, Phys. Rev. Lett. **124**, 252502 (2020).
[9] Z. Y. Zhang, H. B. Yang, M. H. Huang, Z. G. Gan, C. X. Yuan, C. Qi, A. N. Andreyev, M. L. Liu, L. Ma, M. M. Zhang, Y. L. Tian, Y. S. Wang, J. G. Wang, C. L. Yang, G. S. Li, Y. H. Qiang, W. Q. Yang, R. F. Chen, H. B. Zhang, Z. W. Lu *et al.*, Phys. Rev. Lett. **126**, 152502 (2021).
[10] M. Huang, Z. Gan, Z. Zhang, L. Ma, J. Wang, M. Zhang, H. Yang, C. Yang, X. Huang, Z. Zhao, S. Xu, L. Chen, X. Wen,

Y. Niu, C. Yuan, Y. Tian, Y. Wang, J. Wang, M. Liu, Y. Qiang *et al.*, Phys. Lett. B **834**, 137484 (2022).
[11] L. Sheng, Q. Hu, H. Jia, Z. Zhang, Z. Chai, B. Zhao, Y. Zhang, Z. Gan, Y. He, and J. Yang, Nucl. Instrum. Methods Phys. Res. A **1004**, 165348 (2021).
[12] S. Xu, Z. Zhang, Z. Gan, M. Huang, L. Ma, J. Wang, M. Zhang, H. Yang, C. Yang, Z. Zhao, X. Huang, L. Chen, X. Wen, H. Zhou, H. Jia, L. Sheng, J. Wu, X. Peng, Q. Hu, J. Yang *et al.*, Nucl. Instrum. Methods Phys. Res. A **1050**, 168113 (2023).
[13] Z. Zhang, L. Ma, Z. Gan, M. Huang, T. Huang, G. Li, X. Wu, G. Jia, L. Yu, H. Yang, Z. Sun, X. Zhou, H. Xu, and W. Zhan, Nucl. Instrum. Methods Phys. Res. B **317**, 315 (2013).
[14] M. Zhang, H. Yang, Z. Gan, Z. Zhang, M. Huang, L. Ma, C. Yang, C. Yuan, Y. Wang, Y. Tian, H. Zhou, S. Huang, X. He, S. Wang, W. Xu, H. Li, X. Xu, J. Wang, H. Yang, L. Duan *et al.*, Phys. Lett. B **800**, 135102 (2020).
[15] M. M. Zhang, Y. L. Tian, Y. S. Wang, Z. Y. Zhang, Z. G. Gan, H. B. Yang, M. H. Huang, L. Ma, C. L. Yang, J. G. Wang, C. X. Yuan, C. Qi, A. N. Andreyev, X. Y. Huang, S. Y. Xu, Z. Zhao, L. X. Chen, J. Y. Wang, M. L. Liu, Y. H. Qiang *et al.*, Phys. Rev. C **106**, 024305 (2022).
[16] V1724 and VX1724 user manual, https://www.caen.it/.
[17] NNDC National Nuclear Data Center, Chart of Nuclides, https://www.nndc.bnl.gov/nudat2.
[18] J. Heredia, A. Andreyev, S. Antalic, S. Hofmann, D. Ackermann, V. Comas, S. Heinz, F. Heßberger, B. Kindler, J. Khuyagbaatar *et al.*, Eur. Phys. J. A **46**, 337 (2010).
[19] K. Eskola, P. Kuusiniemi, M. Leino, J. F. C. Cocks, T. Enqvist, S. Hurskanen, H. Kettunen, W. H. Trzaska, J. Uusitalo, R. G. Allatt, P. T. Greenlees, and R. D. Page, Phys. Rev. C **57**, 417 (1998).
[20] H. B. Yang, Z. G. Gan, Z. Y. Zhang, M. H. Huang, L. Ma, M. M. Zhang, C. L. Yang, Y. L. Tian, Y. S. Wang, H. B. Zhou, X. J. Wen, J. G. Wang, Z. Zhao, S. Y. Xu, L. X. Chen, X. Y. Huang, C. X. Yuan, Y. F. Niu, H. R. Yang, W. X. Huang *et al.*, Phys. Rev. C **106**, 064311 (2022).
[21] J. F. Ziegler, M. Ziegler, and J. Biersack, Nucl. Instrum. Methods Phys. Res. B **268**, 1818 (2010), 19th International Conference on Ion Beam Analysis.
[22] K. H. Schmidt, C. C. Sahm, K. Pielenz, and H. G. Clerc, Z. Phys. A: At. Nucl. **316**, 19 (1984).
[23] H. B. Zhou, Z. Y. Li, Z. G. Gan, Z. Y. Zhang, H. Yao, N. Wang, H. B. Yang, L. Ma, M. H. Huang, C. L. Yang, M. M. Zhang, Y. L. Tian, Y. S. Wang, X. H. Zhou, and J. L. Tian, Phys. Rev. C **105**, 024328 (2022).
[24] N. Wang and L. Guo, Phys. Lett. B **760**, 236 (2016).
[25] R. du Rietz, E. Williams, D. J. Hinde, M. Dasgupta, M. Evers, C. J. Lin, D. H. Luong, C. Simenel, and A. Wakhle, Phys. Rev. C **88**, 054618 (2013).
[26] R. Bass, Phys. Rev. Lett. **39**, 265 (1977).
[27] W. Reisdorf, Z. Phys. A: At. Nucl. **300**, 227 (1981).
[28] W. Reisdorf and M. Schädel, Z. Phys. A: Hadrons Nucl. **343**, 47 (1992).
[29] S. Cohen, F. Plasil, and W. Swiatecki, Ann. Phys. **82**, 557 (1974).
[30] A. N. Andreyev, D. Ackermann, S. Antalic, I. G. Darby, S. Franchoo, F. P. Heßberger, S. Hofmann, M. Huyse, P. Kuusiniemi, B. Lommel, B. Kindler, R. Mann, G. Münzenberg, R. D. Page, S. Saro, B. Sulignano, B. Streicher, K. Vande Vel, P. Van Duppen, and D. R. Wiseman, Phys. Rev. C **72**, 014612 (2005).
[31] L. Ma *et al.* (to be published).